Konrad-Zuse-Zentrum für Informationstechnik Berlin
Takustraße 7, D-14195 Berlin

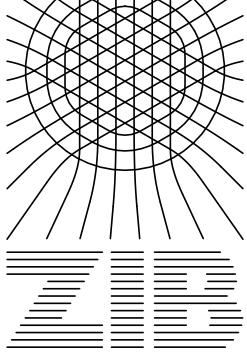

Ulrich Maas[1] Ulrich Nowak

An adaptive method of lines for the simulation of complex laminar combustion processes

[1] Institut für Technische Verbrennung, Universität Stuttgart
Pfaffenwaldring12, 70569 Stuttgart, Germany

Preprint SC 96–56 (December 1996)

An adaptive method of lines for the simulation of complex laminar combustion processes

Ulrich Maas
Institut für Technische Verbrennung, Universität Stuttgart
Pfaffenwaldring12, 70569 Stuttgart, Germany

Ulrich Nowak
Konrad-Zuse-Zentrum für Informationstechnik
Takustr. 7, 14195 Berlin, Germany

Abstract

For the simulation of one-dimensional flame configurations reliable numerical tools are needed which have to be both highly efficient (large number of parametric calculations) and at the same time accurate (in order to avoid numerical errors). This can only be accomplished using fully adaptive discretization techniques both in space and time together with a control of the discretization error.

We present a method which accomplishes this task. It is based on an adaptive MOL (method of lines) treatment. Space discretization is done by means of finite difference approximations on non-uniform grids. Time is discretized by the linearly-implicit Euler method. In order to control the discretizations errors an extrapolation procedure is used in space and time. Results are presented for simple laser-induced ignition processes. The method, however can be applied to other combustion processes, too.

1 Introduction

One of the ultimate goals in CFD (computational fluid dynamics) is the reliable numerical simulation of turbulent, reacting, three-dimensional multi-phase flows like combustion processes [1–3]. However, up to now we are far away from this goal, and even within the next decades it will be impossible to perform DNS (direct numerical simulations) of practical combustion systems. Thus, models are devised which simplify both the description of the turbulence, the physical processes, and the chemical reaction. The development of such models is based on numerous parametric studies of simple one-dimensional reacting flow calculations such as the calculation of laminar flamelets, studies on the evaporation and combustion of single droplets, or the description of simple catalytic combustion processes (see, e.g., [2] for references). The information obtained from these calculations is then used to derive simplified sub-models for the overall CFD-calculation.

Typical one-dimensional simulations nowadays require less than one hour on available workstations. However in order to set up, e.g., laminar flamelet libraries, the results of more than 1000 such laminar flame calculations have to be performed and the results stored for subsequent use in turbulent flame calculations. Thus, it is evident that efficient numerical methods have to be used for the laminar flame simulations. Furthermore, the results have to be reliable, and the numerical errors should be well known and kept beyond a reasonable limit.

In order to meet these requirements, adaptive numerical methods for both space and time discretization have to be used together with a reliable error estimation. In this paper we present such a method. It is based on an adaptive MOL (method of lines) treatment. Space discretization is done by means of finite difference approximations on non-uniform grids. Time is discretized by the linearly-implicit Euler method. In order to control the discretizations errors an extrapolation procedure is used in space and time. This method is applied to a simple test case, namely a laser-induced ignition process.

2 Mathematical Model

2.1 Governing Equations of reacting flows

Mathematical simulation of chemically reacting multi-component compressible flows is performed by solving the corresponding system of conservation equations for mass, momentum, energy, and species masses (Navier-Stokes equations) which may be written as [4–6]:

$$\frac{\partial \rho}{\partial t} + \mathrm{div}\ (\rho \vec{v}) = 0 \tag{1}$$

$$\rho \frac{\partial \vec{v}}{\partial t} + \rho \vec{v} \mathrm{grad}\, \vec{v} + \mathrm{div}\, \overline{\overline{p}} = \rho \vec{g} \tag{2}$$

$$\rho \frac{\partial u}{\partial t} + \rho \vec{v} \mathrm{grad}\, u + \mathrm{div}\, \vec{q} + \overline{\overline{p}} : \mathrm{grad}\, \vec{v} = \omega_h \tag{3}$$

$$\rho\frac{\partial \underline{w}}{\partial t} + \rho\vec{v}\mathrm{grad}\,\underline{w} + \mathrm{div}\,\vec{\underline{j}} \;=\; \underline{\Omega} \tag{4}$$

together with the equation of state $p = p\,[h, \rho, \underline{w}]$, which is in many cases given by the ideal gas law

$$p = \frac{\rho}{\overline{\overline{M}}}RT. \tag{5}$$

In these equations t denotes the time, ρ the density, $\vec{v}$ the velocity vector, p the pressure, $\overline{\overline{p}}$ the pressure tensor, $\vec{g}$ the gravitational acceleration, u the specific internal energy, $\vec{q}$ the heat flux density, ω_h a source term for energy (e.g., due to radiation), $\underline{w}$ the n_s-dimensional vector of mass fractions of the n_s chemical species, $\underline{\Omega}$ the n_s-dimensional vector of (mass scale) chemical rates of formation of the n_s chemical species, $\overline{M}$ the mean molar mass of the mixture, T the temperature, R the universal gas constant, $\vec{\underline{j}}$ the n_s-dimensional vector of the diffusion flux densities of the species relative to the center of mass, and : the two-fold contraction of two tensors.

The transport terms $\overline{\overline{p}}$, $\vec{\underline{j}}$ and $\vec{q}$, which are needed to close the system, are functions of the thermokinetic state of the system and of the gradients of the primitive variables $\vec{v}$, T, $\underline{x}$, and p [4–6] ($\underline{x}$ = vector of mole fractions). In their general form they can be written as [7]:

$$\overline{\overline{p}} = p\overline{\overline{E}} - \mu\left\{(\mathrm{grad}\,\vec{v}) + (\mathrm{grad}\,\vec{v})^T\right\} - \left(\kappa - \frac{2}{3}\mu\right)(\mathrm{div}\,\vec{v})\,\overline{\overline{E}} \tag{6}$$

$$\begin{aligned} \vec{\underline{j}}_i &= M_x^j\mathrm{grad}\underline{x} + M_T^j\mathrm{grad}T + M_p^j\mathrm{grad}p \\ q &= M_x^q\mathrm{grad}\underline{x} + M_T^q\mathrm{grad}T + M_p^q\mathrm{grad}p, \end{aligned} \tag{7}$$

where the M are given by:

$$\begin{array}{lllllll} M_x^j &=& -\overline{\overline{\rho}}\,\overline{\overline{D}} & & M_x^q &=& -\left(\underline{h}^T\overline{\overline{\rho}} + p\underline{\chi}^T\right)\overline{\overline{D}} \\ M_T^j &=& -\overline{\overline{\rho}}\,\overline{\overline{D}}\frac{\chi}{T} & & M_T^q &=& -\left(\underline{h}^T\overline{\overline{\rho}} + p\underline{\chi}^T\right)\overline{\overline{D}}\frac{\chi}{T} - \lambda \\ M_p^j &=& -\overline{\overline{\rho}}\,\overline{\overline{D}}\frac{\underline{x}-\underline{w}}{p} & & M_p^q &=& -\left(\underline{h}^T\overline{\overline{\rho}} + p\underline{\chi}^T\right)\overline{\overline{D}}\frac{\underline{x}-\underline{w}}{p} \end{array} \tag{8}$$

In these equations $\overline{\overline{E}}$ denotes the unit tensor, $\overline{\overline{D}}$ the diffusion matrix, λ the heat conductivity of the mixture, $\overline{\overline{\rho}}$ the diagonal matrix formed by the partial densities ρ_i, $\underline{x}$ the vector of mole fractions, $\underline{w}$ the vector of mass fractions, $\underline{\chi}$ the vector of thermal diffusion ratios χ_i, and $\underline{h}$ the vector of specific enthalpies h_i (see [7] for details).

The independent variables in the equation systems above are the time t and the spatial coordinates $\vec{r}$, the dependent variables are ρ, $\vec{v}$, u, and $\underline{w}$.

For a convenient time- and space discretization it is important to rewrite the molecular transport terms such that they are expressed in terms of gradients of the dependent variables ρ, $\vec{v}$, u, and $\underline{w}$. Using straight forward differentiation rules, and using the ideal gas law, we obtain:

$$\begin{array}{lllllll} \mathrm{grad}\,\underline{x} &=& \underline{x}_{\underline{w}}\mathrm{grad}\,\underline{w} & & \underline{x}_{\underline{w}} &=& \overline{M}\left\{\mathrm{diag}(\hat{M}) - \underline{x}\hat{M}^T\right\} \\ \mathrm{grad}\,T &=& T_{\underline{w}}\mathrm{grad}\,\underline{w} + T_u\mathrm{grad}\,u & & T_u &=& \frac{1}{c_v} \qquad T_{\underline{w}} = -\frac{\underline{u}}{c_v} \end{array} \tag{9}$$

In the following we restrict ourselves to a one-dimensional closed chemical reaction system with spatially homogeneous pressure and cartesian geometry. Then the momentum equation has not to be solved, and after a transformation into *Lagrangian* coordinates, the governing equations simplify to [8]:

$$\frac{\partial r}{\partial \eta} = \frac{1}{\rho} \tag{10}$$

$$\frac{\partial p}{\partial \eta} = 0 \tag{11}$$

$$\frac{\partial u}{\partial t} + \frac{\partial q}{\partial \eta} = \frac{\omega_h}{\rho} \tag{12}$$

$$\frac{\partial \underline{w}}{\partial t} + \frac{\partial \underline{j}}{\partial \eta} = \frac{\underline{\Omega}}{\rho}, \tag{13}$$

where η denotes the *Lagrangian* coordinate. The boundary conditions at $\eta = 0$ and $\eta = \eta^m$ are given by

$$\begin{array}{lllllllll} \eta = 0: & r = r^i & \frac{\partial u}{\partial \eta} = 0 & \frac{\partial p}{\partial \eta} = 0 & \frac{\partial \underline{w}}{\partial \eta} = 0 \\ \eta = \eta^m: & \frac{\partial r}{\partial \eta} = \frac{1}{\rho} & \frac{\partial u}{\partial \eta} = 0 & r = r^o & \frac{\partial \underline{w}}{\partial \eta} \quad 0. \end{array} \tag{14}$$

Rewriting the equation system in vector notation yields with $\underline{\psi} = (r, p, u, \underline{w})^T$:

$$A\frac{\partial \psi}{\partial t} + B\frac{\partial \psi}{\partial \eta} + \frac{\partial}{\partial \eta} C \frac{\partial \psi}{\partial \eta} = D \tag{15}$$

with

$$A = \begin{pmatrix} 0 & 0 & 0 & 0 \\ 0 & 0 & 0 & 0 \\ 0 & 0 & 1 & 0 \\ 0 & 0 & 0 & I \end{pmatrix} \qquad B = \begin{pmatrix} 1 & 0 & 0 & 0 \\ 0 & 1 & 0 & 0 \\ 0 & 0 & 0 & 0 \\ 0 & 0 & 0 & 0 \end{pmatrix} \tag{16}$$

$$C = \begin{pmatrix} 0 & 0 & 0 & 0 \\ 0 & 0 & 0 & 0 \\ 0 & M_p^q & M_T^q T_u & M_x^q \underline{x}_{\underline{w}} + M_T^q T_{\underline{w}} \\ 0 & M_p^j & M_T^j T_u & M_x^j \underline{x}_{\underline{w}} + M_T^j T_{\underline{w}} \end{pmatrix} \qquad D = \begin{pmatrix} 1/\rho \\ 0 \\ \omega_h/\rho \\ \Omega/\rho \end{pmatrix} \tag{17}$$

3 An adaptive MOL–method

In short notation the equations (14,15) represent a system of n_{pde} partial differential equations (PDEs) of reaction–diffusion type with possibly mild convection

$$B(x,t,u,u_x)u_t = f(x,t,u,u_x,(D(x,t,u)u_x)_x) \tag{18}$$

$$u(x,t_0) = u_0(x) \tag{19}$$

$$\alpha(x)u + \beta(x,t,u)u_x = \gamma(x,t,u) \text{ or } u_t = \delta(x,t,u) \tag{20}$$

$$x \in [x_L, x_R]\ , \quad t \in [t_0, t_{\text{end}}] \tag{21}$$

Herein, the matrix B may be singular but we assume that, after space discretization, the appearing system of differential–algebraic equations (DAEs) is of index ≤ 1.

For problems of this type an adaptive method–of–lines approach based on extrapolation techniques has been developed recently [9]. The method is implemented in an efficient software package, PDEX1M [10].

The approach starts from a second order finite difference discretization of the spatial derivatives in (14,15) The usual centered approximations on non–uniform grids

$$\mathcal{G} = \{x_L = x_1 < \ldots < x_{n_x} = x_R\} \tag{22}$$

are applied, see e.g. [11]. On uniform grids these finite difference approximations show a quadratic truncation error. On non–uniform grids the local truncation error is formally only linear in the discretization stepsizes $\Delta x_i = x_{i+1} - x_i$. In order to overcome this formal difficulty one may introduce (see e.g. [12]) a sufficiently differentiable virtual grid function $\xi(r)$ which is implicitly defined by the following properties:

$$\begin{aligned} x_i &= \xi(r_i)\ , \quad i = 1, ..., n_x \\ r_i &= (i-1) \cdot \Delta R\ ,\ \Delta R = 1/(n_x - 1)\ , \quad i = 1, \ldots, n_x\ . \end{aligned}$$

By means of this grid function the local truncation error of the space discretization of our problem shows a quadratic error expansion in ΔR.

After space discretization one ends up with a system of differential–algebraic equations (DAEs) of the form

$$\mathbf{B}(\mathbf{u})\mathbf{u}' = \mathbf{f}(t, \mathbf{u})\ . \tag{23}$$

This system is nonlinear, stiff, block structured and large. It can be solved by any standard DAE–solver, e.g. the extrapolation method LIMEX [13]. However, the prescribed accuracy for this integration will bound the error of the solution approximation to system (23) but, in general, not to the original system (14,15). To estimate and control the error from space discretization also one may combine the extrapolation in time of LIMEX with an additional extrapolation in space. In the following, we summarize this extrapolation in space and time.

To discretize in time the modified linearly implicit Euler discretization [13] is applied to (23). One step, say from t_k to $t_{k+1} = t_k + \Delta t$, reads

$$(\mathbf{B}_k - \Delta t \mathbf{A})(\mathbf{u}_{k+1} - \mathbf{u}_k) = \Delta t \mathbf{f}(t_{k+1}, \mathbf{u}_k)\ , \tag{24}$$

where $\mathbf{A}$ is the Jacobian matrix of the residual, $\mathbf{A} = (\mathbf{f} - \mathbf{B}\mathbf{u}')_u$, at $t = t_L \leq t_k$, or a sufficient good approximation of it. This elementary discretization which shows a linear error expansion in Δt is extended to a method of higher order by means of extrapolation in time:

Assume a grid $\mathcal{G}_1$ and associated solution values are given at time t_L. Further, a so–called basic stepsize ΔT and an associated extrapolation stage number s are given. Then one constructs approximations to $\mathbf{u}(t_L + \Delta T)$ using the discretization method (24) with stepsizes $\Delta t_j = \Delta T / n_j$, $j = 1, \ldots, \kappa$, $\kappa = s + 1$, where $\{n_j\}$ is the step number sequence. For the linearly–implicit Euler method the harmonic sequence $\{n_j\} = \{1, 2, 3, \ldots\}$ may be applied. In order to make clear that the original system

has been discretized the approximation obtained with stepsize Δt_j on the grid $\mathcal{G}_1$ may be written as

$$U(x_i, t_L + \Delta T; \Delta R_1, \Delta t_j), i = 1, \ldots, n_x, j = 1, \ldots, \kappa \; . \tag{25}$$

The following expansion describes the essential error behavior of these approximations at $t_R = t_L + \Delta T$

$$\begin{aligned} U(x_i, t_R; \Delta R_1, \Delta t_j) - u(x_i, t_R) &= \sum_{l=1}^{N} e(x_i, t_R) \Delta t_j^l + O(\Delta t_j^{N+1}) & (26) \\ &\quad + O(\Delta R^2) + O(\Delta R^4) \; . & (27) \end{aligned}$$

The leading time error terms are eliminated by extrapolation using the *Aitken–Neville*–scheme

$$\begin{aligned} & j = 1, \ldots, \kappa : & (28) \\ & T_{j,1} = U(x_i, t_R; \Delta R_1, \Delta t_j) & (29) \\ & T_{j,k} = T_{j,k-1} + \frac{T_{j,k-1} - T_{j-1,k-1}}{n_j / n_{j-k+1} - 1} \; , k = 2, \ldots, j \; . & (30) \end{aligned}$$

This extrapolation can be done independently for the approximations at all nodes x_i of the given grid. The norm of the leading approximation error of the $T_{j,k}$ is

$$||T_{j,k} - u(x_i, t_R)|| \doteq C_j \Delta T^{k+1} + O(\Delta R^2)$$

and depends still on the space discretization stepsize ΔR. With

$$\epsilon_t(x_i) = ||T_{j,j-1} - T_{j,j}|| \tag{31}$$

local time error estimates for the approximations $T_{j,j-1}$ are available. Note that the leading time error of this estimate coincides with the leading true error of $T_{j,j-1}$. As the leading space error terms of $T_{j,j}$ and $T_{j,j-1}$ are the same, they cancel in (31).

In order to derive a space error estimate one space extrapolation step is performed. Dropping each second node of the current computational grid (global coarsening) means to replace the basic stepsize ΔR_1 by $\Delta R_2 = 2\Delta R_1$. Now the time integration step is repeated and new approximations

$$u(\bar{x}_i, t_L + \Delta T; \Delta R_2, \Delta t_j) \; , i = 1, \ldots, \bar{n}_x, j = 1, \ldots, \kappa.$$

are available at t_R for $\bar{x}_j \in \mathcal{G}^2 = \{x_1, x_3, \ldots, x_{n_x}\}$. Restricting the fine grid solution (25) to the coarse grid and extrapolating once yields approximations of higher order (with respect to the space discretization stepsize ΔR). With all these values at hand the leading space errors $\epsilon_x(x_i)$ of the fine grid solution at the nodes of the coarse grid can be estimated by a difference similar to (31). Thus, with an appropriate norm, global error estimates ϵ_t and ϵ_x for the leading error terms of the approximations $\{T_{j,j-1}(x_i)\}_{i=1,\ldots,n_x}$ are calculated. The current integrations step is accepted only if the convergence criterion

$$\epsilon_x \leq tol_x \;\; \text{and} \;\; \epsilon_t \leq tol_t$$

is met. Herein, tol_x and tol_t are user prescribed values. In case of failure, the step is repeated with smaller stepsizes.

Note that the whole scheme has variable order in time but only one space extrapolation step – just for the error estimation. Further extrapolation in space would give approximations of higher order but at the nodes of the coarse grid only. In order to proceed the integration starting values at nodes of finer grids are needed and we are left with the problem that high order interpolation on noisy data tends to produce large errors. So just two grid are used. Compared to a usual MOL–treatment without error estimation, all time steps are computed twice. However, the additional work is the computation on the coarse grid. As this computation is done first, an expected failure of the step is cheaply recognized (time error behavior is monitored already during this step).

New stepsizes ΔR and ΔT and a new stage number s are estimated by an extension of the order and stepsize control due to DEUFLHARD [14] for purely time dependent problems. In order to reduce the number of new grid points where a solution approximation must be computed by an interpolation procedure, the choice of a new stepsize ΔR restricted to the values

$$\Delta R^{\text{new}} \in \{2\Delta R^1, \Delta R^1, \Delta R^1/2\}.$$

Besides this global grid adaptation the grid must be adapted locally also. To adapt the spatial grid locally the following equidistribution procedure is used additionally. Recall that local error estimates $\epsilon_x(\bar{x}_i)$ are available. Although the global estimate ϵ_x has passed the convergence test, some of the local estimates may be larger than tol_x and at some nodes $\epsilon^x(\bar{x}_i) \ll tol_x$ may hold. On an optimal grid the local errors would be equidistributed and the following algorithm aims at this. Threshold values are defined by

$$\begin{aligned}
\sigma^+ &= \epsilon^x_{\max}\ ,\ \text{if } \varepsilon^x_{\max} \le tol_x \\
\sigma^+ &= \sqrt{\epsilon^x_{\max} \cdot tol_x}\ ,\ \ \text{if } \epsilon^x_{\max} > \text{tol}_x \\
\sigma^- &= \frac{1}{6}\text{tol}_x\ ,
\end{aligned}$$

with $\epsilon^x_{\max} = \max\{\epsilon^x_i\}$. The general grid adaptation rules are

- if $\epsilon^x_i < \sigma^-$: node x_i may be eliminated
- if $\epsilon^x_i \ge \sigma^-$: node x_i cannot be eliminated
- if $\epsilon^x_i > \sigma^+$: subdivide Δx_{i-1} and Δx_i.

Some heuristical restrictions are imposed to regularize the adaptation and the new grid.

4 Results

The method described above has been used to simulate a laser-induced ignition of a hydrogen-oxygen-mixture (see [8] for details on the physics of such laser-induced

ignition processes). The system investigated here corresponds to a large container with a stoichiometric hydrogen-oxygen mixture at 0.3 bar and 298 K, which is ignited by a laser light sheet. The detailed mechanism used in the simulations consists of 8 chemical species reacting in 37 reactions [8]. Thus 8 species conservation equations have to be solved besides the conservation equations for total mass and energy. Figures 1-4 show the time evolution of the ignition process. Plotted are temperature and some species profiles versus the spatial coordinate and the time. Due to the symmetry of the problem only half of the physical domain has been calculated and plotted. During the irradiation by the laser sheet (within the first 100 μs) the temperature is increased to about 1200 K in the source volume (in the region around $r = 0$). After a short induction period the system starts to ignite, which can be seen from the rapid increase of the temperature. Then a flame front is formed, which propagates into the unburnt mixture.

It can be seen from the different plots that simulations of ignition processes demand numerical solution methods adaptive both in space and time. In Figure 5 the automatically selected grid is plotted in a x-t–plan. During the induction period a very coarse grid can be used. As the system ignites the local refinement process produces a fine grid at the space interval with high spatial activity. This zone with small space discretization intervals nicely follows the propagating fronts in temperature and species concentration.

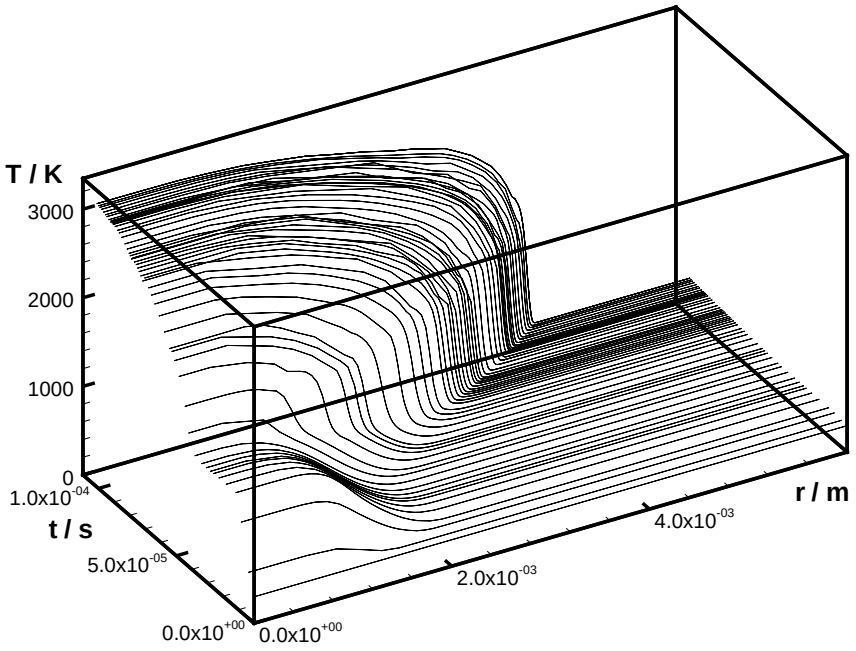

Figure 1: Profiles of temperature during a laser-induced ignition of a hydrogen-oxygen mixture

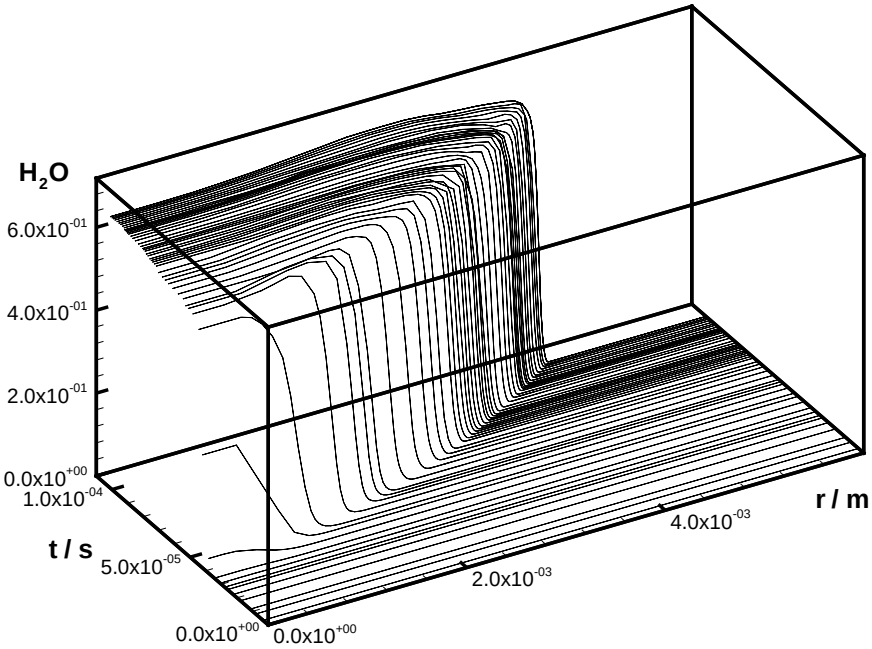

Figure 2: Profiles of H_2O mass fractions during a laser-induced ignition of a hydrogen-oxygen mixture

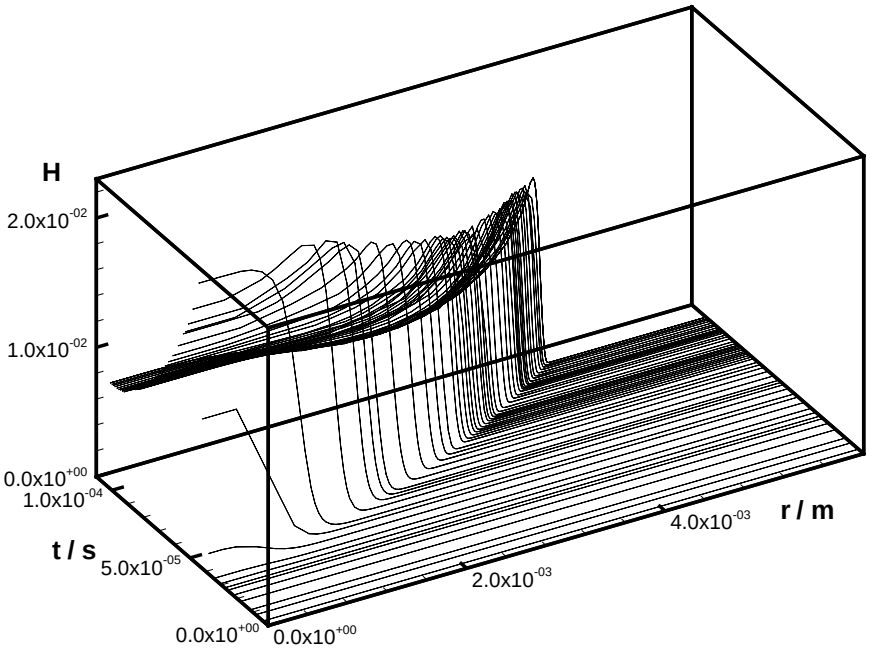

Figure 3: Profiles of H mass fractions during a laser-induced ignition of a hydrogen-oxygen mixture

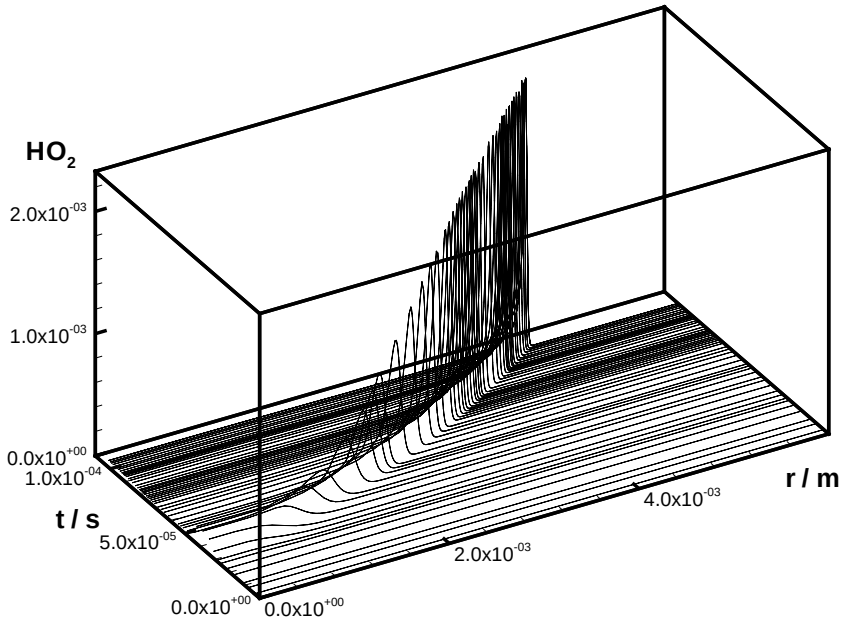

Figure 4: Profiles of HO2 mass fractions during a laser-induced ignition of a hydrogen-oxygen mixture

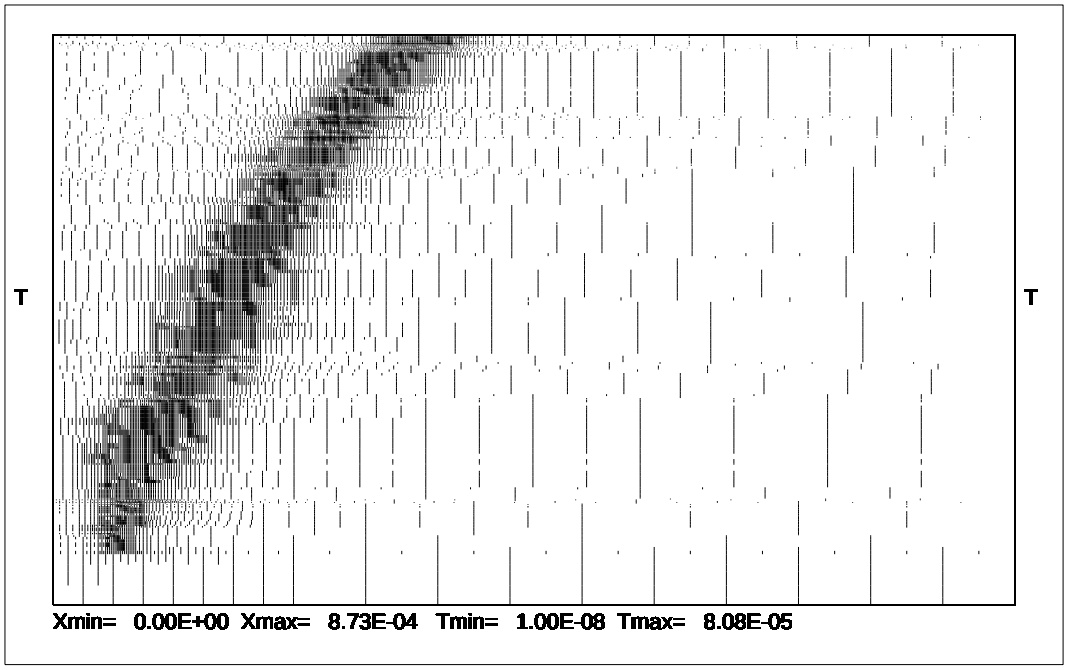

Figure 5: Adaptive grid in a x-t–plan

References

[1] S. B. Pope. *Computations of Turbulent Combustion: Progress and Challenges.* 23rd Symposium (International) on Combustion. The Combustion Institute, Pittsburgh, 1990.

[2] J. Warnatz, U. Maas, and R. W. Dibble. *Combustion.* Springer-Verlag Berlin Heidelberg New York, 1996.

[3] P. A. Libby and F. A. Williams (eds.). *Turbulent Reactive Flows.* Springer, New York, 1980.

[4] J. O. Hirschfelder and C. F. Curtiss. *Theory of Propagation of Flames. Part I: General Equations.* 3rd Symposium (International) on Combustion, Williams and Wilkins, Baltimore, 1949.

[5] J.O. Hirschfelder, C.F. Curtiss, and R.B. Bird. *Molecular Theory of Gases and Liquids.* Wiley, New York, 1954.

[6] R.B. Bird, W.E. Stewart, and E.N. Lightfoot. *Transport Phenomena.* Wiley Interscience, New York, 1960.

[7] A. Ern and V. Giovangigli. *Multicomponent Transport Algorithms.* Lecture Notes in Physics. Springer, Berlin, Heidelberg, New York, 1994.

[8] U. Maas and J. Warnatz. Ignition processes in hydrogen-oxygen mixtures. *Combustion and Flame*, 74:53, 1988.

[9] U. Nowak. A fully adaptive mol-treatment of parabolic 1-D problems with extrapolation techniques. *Applied Numerical Mathematics*, 20:129–145, 1996.

[10] U. Nowak. PDEX1M - a software package for the numerical simulation of parabolic systems in one space dimension. In F. Keil, W. Mackens, H.Voss, and J. Werther, editors, *Scientific Computing in Chemical Engineering.* Springer, 1996.

[11] R.F. Sincovec and N.K. Madsen. Software for nonlinear partial differential equations. *ACM Trans. Math. Software*, 1, no. 3:232–260, 1975.

[12] R.K. de Rivas. On the use of nonuniform grids in finite difference equations. *J. Comput. Phys.*, 10:202–210, 1972.

[13] P. Deuflhard and U. Nowak. Extrapolation integrators for quasilinear implicit ode's. In P. Deuflhard and B. Enquist, editors, *Large Scale Scientific Computing. Progress in Scientific Computing Vol. 7.* Birkhäuser, Boston, Basel, Stuttgart, 1987.

[14] P. Deuflhard. Order and stepsize control in extrapolation methods. *Numerical Mathematics*, 41:399–422, 1983.